Published in final edited form as:
Aging Cell. 2011 October ; 10(5): 879–884. doi:10.1111/j.1474-9726.2011.00733.x.

The Rieske oxygenase DAF-36 functions as a cholesterol 7-desaturase in steroidogenic pathways governing longevity

Joshua Wollam[1,2,3], **Lilia Magomedova**[5], **Daniel B Magner**[3], **Yidong Shen**[3], **Veerle Rottiers**[1], **Daniel L Motola**[6], **David J Mangelsdorf**[6], **Carolyn L Cummins**[5], and **Adam Antebi**[1,2,3,4,*]

Joshua Wollam: JWollam@age.mpg.de; Lilia Magomedova: Lilia.Magomedova@utoronto.ca; Daniel B Magner: DMagner@age.mpg.de; Yidong Shen: YShen@age.mpg.de; David J Mangelsdorf: Davo.Mango@UTSouthwestern.edu; Carolyn L Cummins: Carolyn.Cummins@utoronto.ca

[1]Dept of Molecular and Cellular Biology, Huffington Center on Aging, Baylor College of Medicine, One Baylor Plaza, Houston, TX 77030

[2]Interdepartmental Program in Cell and Molecular Biology, Huffington Center on Aging, Baylor College of Medicine, One Baylor Plaza, Houston, TX 77030

[3]Max Planck Institute for Biology of Ageing, Gleueler Str. 50a, 50931 Cologne, Germany

[4]Cologne Excellence Cluster on Cellular Stress Responses in Aging Associated Diseases (CECAD), University of Cologne, 50674 Cologne, Germany

[4]Dept of Pharmaceutical Sciences, University of Toronto, 144 College Street, Toronto, Ontario M5S 3M2, Canada

[5]Dept. of Pharmacology and Howard Hughes Medical Institute, University of Texas Southwestern Medical Center at Dallas, Dallas, TX 75930

Summary

Bile acids are cholesterol-derived signaling molecules that regulate mammalian metabolism through sterol-sensing nuclear receptor transcription factors. In *C. elegans*, bile acid-like steroids called dafachronic acids (DAs) control developmental timing and longevity by activating the nuclear receptor DAF-12. However, little is known about the biosynthesis of these molecules. Here we show that the DAF-36/Rieske oxygenase works at the first committed step, converting cholesterol to 7-dehydrocholesterol. Its elucidation as a cholesterol 7-desaturase provides crucial biochemical evidence that such oxygenases are key steroidogenic enzymes. By controlling DA production, DAF-36 regulates DAF-12 activities for reproductive development and longevity, and may illuminate related pathways in metazoans.

Keywords

bile acid; nuclear receptor; endocrine signaling; hormone; development; aging

Introduction

Cholesterol homeostasis is critical to animal health and disease, and levels are tightly controlled by the balance of dietary intake, *de novo* synthesis, and catabolism. Cholesterol is metabolized to oxysterols, bile acids and steroids, which serve as signaling molecules for

*Correspondence: AAntebi@age.mpg.de, Tel: +49-221-4788-9681.

Author Contributions: JW, LM, DBM, YS, VR, DLM and AA conducted experiments, AA, CLC, and DJM supervised projects, and JW and AA wrote the paper.

sterol sensing nuclear hormone receptors, transcription factors that respond to cognate ligands to regulate gene expression. These receptors, including the liver X receptor (LXR), farnesoid X receptor (FXR), and vitamin D receptor (VDR), regulate complex networks governing cholesterol, lipid, and glucose homeostasis, as well as aspects of development and reproduction (Wollam & Antebi 2011).

Sterol homeostasis is less well understood in model invertebrates such as *C. elegans*, yet its study through metabolic genetics can illuminate novel pathways of regulation and organismal physiology. *C. elegans* cannot synthesize cholesterol *de novo*, but requires dietary cholesterol for development, molting, and reproduction (Chitwood 1999). Biochemical studies reveal that cholesterol is first converted to 7-dehydrocholesterol and lathosterol, in steps that are intriguingly opposite of mammalian cholesterol biosynthesis, but the functions of these metabolites and the enzymes making them have remained elusive.

Important clues to their roles have come from the identification of bile acid-like steroids, called the dafachronic acids, which are thought to be derived from these precursors (Motola *et al.* 2006). At least two endogenous ligands, Δ^4- and Δ^7-dafachronic acid, act through the nuclear receptor DAF-12 (a homolog of vertebrate FXR, LXR and VDR) to regulate developmental timing, entry into a long-lived larval stage called the dauer diapause, as well as adult longevity in response to signals from the gonad (Antebi *et al.* 2000; Gerisch *et al.* 2007; Bethke *et al.* 2009). More generally, components of the endocrine network controlling dauer formation, such as insulin/IGF signaling, have emerged as important regulators of life span in mammals, though it is unknown whether bile acids also modulate mammalian longevity (Kenyon 2010). The DAF-12-related nuclear receptors and DA signaling pathways are conserved in evolutionarily distant parasitic nematodes, and importantly, regulate exit from the infective stage (Ogawa *et al.* 2009; Wang *et al.* 2009). Thus, dissecting the pathways leading to DA production may not only illuminate the biology of aging, but also help identify targets for anti-helminthic therapeutics.

Relatively little is known about the pathways that govern DA synthesis, regulation, and ligand specificity. A cytochrome P450, DAF-9, functions at the last step in the DA biosynthetic pathway, oxidizing the cholesterol side chain of 3-keto steroids (lathosterone and 4-cholesten-3-one) to give Δ^7-DA and Δ^4-DA, respectively (Motola *et al.* 2006), a chemistry analogous to mammalian CYP27A1 in mammalian bile acid synthesis (Russell 2003). Null mutations of *daf-9* abolish DA production entirely, and animals constitutively enter the dauer diapause with complete penetrance (Gerisch *et al.* 2001; Jia *et al.* 2002). HSD-1, a 3-hydroxysteroid-dehydrogenase homolog with weaker phenotypes than *daf-9*, is proposed to make the 3-keto steroid 4-cholesten-3-one in the synthesis of Δ^4-DA, but there is as of yet no biochemical evidence for this activity (Patel *et al.* 2008; Dumas *et al.* 2010). DAF-36 is a Rieske-like oxygenase implicated in DA biosynthetic pathways, the loss of which also results in less severe phenotypes than *daf-9*, suggesting it acts in early biosynthetic branches that converge on DAF-9/CYP450 (Rottiers *et al.* 2006). The identification of *C. elegans* DAF-36 and *Drosophila neverland* provided the first evidence that such enzymes function in animal steroidogenic pathways (Yoshiyama *et al.* 2006), but their general role in metazoa and their biochemical activity remain uncharacterized. Here we show that DAF-36 works in the very first steps of nematode cholesterol metabolism, converting cholesterol to 7-dehydrocholesterol. As such, *daf-36* could be a node of regulation for the partitioning of cholesterol to steroidogenic and bile acid pathways. By controlling the activity of DAF-12/FXR, it thereby influences developmental timing and longevity, and may also prove to be a promising therapeutic target against pathogenic nematodes.

Results

daf-36 mutants exhibit phenotypes typical of mild DA deficiency, forming dauer larvae constitutively at 27°C (Daf-c), and exhibiting gonadal cell migration (Mig) defects at lower temperatures (Rottiers *et al.* 2006). To determine where in the hormone biosynthetic pathways DAF-36 might act, we performed sterol feeding experiments to rescue these phenotypes. We reasoned that mutants blocked in hormone production should be rescued by compounds lying downstream or parallel to the block, but not by those lying upstream.

Previously we showed that *daf-36* Daf-c phenotypes were rescued by various sterols (Rottiers *et al.* 2006), which we verified here. 7-Dehydrocholesterol, lathosterol, lathosterone, Δ^7-DA, as well as 4-cholesten-3-one and Δ^4-DA, rescued Daf-c phenotypes at 27°C, but not cholesterol (Figure 1A, Table S1). This suggests that cholesterol lies upstream of the *daf-36* step, while other compounds lie downstream or in parallel. The conversion of cholesterol to 7-dehydrocholesterol is an important initial step in nematode cholesterol metabolism, suggesting that DAF-36 itself could act early at this step. By contrast, the *daf-9(k182)* hypomorphic allele was fully rescued by the DAs only, consistent with DAF-9/CYP450 working at the last step (Table S1). Additionally, 7-dehydrocholesterol, but not cholesterol, could also rescue *daf-36* gonadal Mig phenotypes (Table S1). It is noteworthy that *daf-36* animals grown on pure cholesterol (≥99%) had more severe Mig phenotypes (69%) than those grown on the less pure compound (≥92.5% cholesterol, 0% Mig), presumably due to contaminating sterols.

To independently measure *daf-36* physiologic activity, we examined its influence on *daf-9/CYP450* regulation. *daf-9/CYP450* transcription is tightly regulated in the hypodermis, a syncitial epidermal tissue surrounding the worm (Gerisch & Antebi 2004; Mak & Ruvkun 2004). *daf-9* null mutant animals lacking DA are Daf-c with complete penetrance, and hypodermal *daf-9::gfp* expression is undetectable. By contrast, mutations thought to partially block DA production, such as *daf-9* hypomorphs or *daf-36* null mutants, often provoke visible upregulation of hypodermal *daf-9::gfp* and dauer bypass. Such upregulation is hypothesized to reflect homeostatic feedback by hormone. To test directly whether *daf-9::gfp* levels are regulated by hormonal feedback, we fed the DAs and their proposed precursors to *daf-36* mutants. Mutants cultured on vehicle resulted in upregulation of hypodermal *daf-9::gfp* compared to WT controls (Figure 1B–C). Supplementation with the DAs or 7-dehydrocholesterol, but not cholesterol, dramatically reversed *daf-9::gfp* upregulation. These results demonstrate that DA serves as a negative feedback signal on the *daf-9* promoter, and support the hypothesis that *daf-36* defects arise from failure to convert cholesterol to 7-dehydrocholesterol.

To further test this hypothesis, we examined sterol profiles from mutants. We grew animals in bulk liquid culture, extracted lipids, and analyzed sterols by LC/MS/MS. Strikingly, *daf-36* mutants lacked 7-dehydrocholesterol, revealing a 6.5-fold decrease relative to WT (Figure 2A–B). Animals grown on solid media and analyzed by GC/MS/MS gave a similar profile. Mutant extracts were deficient in the putative product, 7-dehydrocholesterol, and accumulated the putative precursor, cholesterol, by 3-fold (Figure 2C–D). The DAF-12 ligand, Δ^7-DA, was also undetectable in *daf-36* mutants, while Δ^4-DA was below the detection limit in both WT and mutants (Figure 2E, data not shown). Thus, DAF-36 supports production of Δ^7-DA, and specifically acts in the metabolism of cholesterol to 7-dehydrocholesterol.

To analyze DAF-36 biochemical activities, we expressed *daf-36* cDNA in cultured *Sf9* cells and isolated microsomes. We found that the presence of DAF-36 resulted in a significant increase in 7-dehydrocholesterol relative to controls (Figure 3A–B), and extracts from these

microsomes rescued the Daf-c phenotypes of *daf-36* mutants (Figure 3C). We conclude that DAF-36 converts cholesterol to 7-dehydrocholesterol, and serves as a cholesterol 7-desaturase (Figure 3D).

If *daf-36* mutants diminish Δ^7-DA production, expression of DAF-12 target genes should also be reduced. To test this, we examined two direct DAF-12 target genes, the microRNAs *mir-84* and *mir-241*, by qPCR (Bethke *et al.* 2009). Both transcripts were significantly reduced by about 50% in *daf-36* mutants, illustrating perturbation of the DAF-12 transcriptional response (Figure 4).

Discussion

In this work we demonstrate that the DAF-36/Rieske oxygenase functions as a cholesterol 7-desaturase involved in the production of the bile acid-like steroid, Δ^7-DA. By controlling DA production, DAF-36 regulates DAF-12/FXR transcriptional activity and hence developmental timing and longevity. This study provides crucial biochemical evidence that such enzymes play an important role in the first steps of cholesterol metabolism towards the production of bioactive steroids.

Several lines of evidence show that DAF-36 is a cholesterol 7-desaturase responsible for the production of 7-dehydrocholesterol, thereby impacting DA synthesis and DAF-12 activity. First, *daf-36* mutants exhibit the phenotypic profile associated with DA deficiency, including Daf-c phenotypes, gonadal Mig defects, and abrogated longevity in animals lacking germline stem cells (Rottiers *et al.* 2006). *daf-36* mutants also exhibit reduced expression of the DAF-12 dependent target genes, the *let-7* related microRNAs, *mir-84* and *mir-241*, which function in developmental timing (Bethke *et al.* 2009). Second, sterol feeding experiments reveal that Δ^7-DA and the early precursor, 7-dehydrocholesterol, rescue *daf-36* mutant phenotypes, whereas cholesterol does not. Such sterol supplementation experiments implicate *daf-36* as an important first step in nematode cholesterol catabolism, the conversion of cholesterol to 7-dehydrocholesterol.

Direct evidence for this activity stems from biochemical analysis. Lipid extracts from *daf-36* mutants accumulate the proposed precursor, cholesterol, and are dramatically deficient in the predicted product, 7-dehydrocholesterol, as well as the end product of the pathway, Δ^7-DA. The fact that *daf-36* mutants have undetectable Δ^7-DA, yet have weaker phenotypes than *daf-9*/*CYP450* mutants, implies that residual amounts of a known DAF-12 ligand or that alternate ligand(s) are present. Finally, microsomes expressing the DAF-36 protein in a heterologous system produce 7-dehydrocholesterol, establishing DAF-36 as a cholesterol 7-desaturase. It has long been noted that several nematode sterols contain the Δ^7 double bond (Chitwood 1999); DAF-36 activity is the likely source of such modifications. In the future it will be interesting to dissect the co-factors and molecular mechanism underlying this activity.

Rieske-like oxygenases are non-heme iron-dependent oxygenases that carry out diverse chemical reactions, including oxygenation and desaturation of ring structures (Bugg & Ramaswamy 2008). Studied most intensively in bacteria, including *Mycobacterium tuberculosis*, the Rieske oxygenase *kshA* has been shown to function as a 9α-hydroxylase on 3-ketosteroids and contributes to pathogenesis (Hu *et al.* 2010). Among eukaryotes, the Rieske-like oxygenases are conserved in plants, worms, insects, sea urchins, amphibians, fish, and birds, but have not been studied in vertebrates. Functional studies in worms and flies are amongst the first to ascribe a role of such enzymes to steroidogenesis. Like DAF-36, *Drosophila neverland* is implicated in the first steps of ecdysone synthesis, and is involved in the conversion cholesterol to 7-dehydrocholesterol, based on sterol

supplementation experiments (Yoshiyama *et al.* 2006). In *C. elegans*, 7-dehydrocholesterol not only supports DA production, but can serve as a source of sterols for growth and molting (Chitwood 1999). By inference, DAF-36 may contribute to sterol pools for these other processes. Of particular interest are DAF-36 homologs in pathogenic nematodes, as they may present novel therapeutic targets to combat animal and plant parasitism (Wang *et al.* 2009).

Although mammals lack a clear DAF-36 homolog, it remains possible that the function has been assumed by another gene product. Rieske domains and non-heme iron binding motifs are found in different proteins but not together, raising the possibility that a DAF-36-like function could be separated. Extracts from the guinea pig gut have the ability to convert cholesterol to 7-dehydrocholesterol (Glover *et al.* 1952). The first step of mammalian bile acid synthesis entails hydroxylation of the 7-position of cholesterol (Russell 2003). Speculatively, modification of the 7-position, either by hydroxylation or desaturation, may be a conserved feature in the first step of partitioning cholesterol to bile acid production. As such, we hypothesize *daf-36* may be a key point of control, and indeed, insulin signaling is known to regulate its expression (Rottiers *et al.* 2006). Ultimately it will be interesting to understand the biochemical activities and physiologic functions of potential vertebrate homologs, particularly with respect to steroidogenesis and bile acid metabolism, and how such bioactive steroids impact longevity.

Experimental Procedures

C. elegans Growth Conditions

Worms were grown on NGM agar seeded with the *E. coli* bacteria strain OP50 at 20°C unless noted otherwise. NGM contains 5 μg/mL cholesterol (≥92.5%, Sigma-Aldrich, St. Louis, MO), which is omitted in low cholesterol conditions. Rescue with pure steroids was performed as described (Rottiers *et al.* 2006).

Microsomal Incubations

Sf9 cells were cultured and harvested 60 hours post-infection and microsomes prepared as described (Motola *et al.* 2006). Microsomes expressing DAF-36 and human oxidoreductase (hOR) or hOR alone were thawed on ice, and brought to 0.5 mg/mL in either 0.1 M KPO_4 buffer alone or including a NADPH regenerating system (50 U/ml isocitrate dehydrogenase, 0.1 M isocitrate and 0.1 M $MgCl_2$). Substrates were added at 100 μM in 0.5 mL total volume, preincubated for 3 minutes at 37°C and reacted with 1 mM NADPH for 16 hours at 37°C. Reactions were processed by extracting twice with 2 mL methyl tert-butyl ether (MTBE), and drying under nitrogen. In some experiments, microsomes were processed without incubation with substrates. 0.5 μg of cholesterol-d_7 was added as an internal standard for extractions. For rescues, extracts were resuspended in 50 μL methanol, mixed with 5X concentrated OP50, vacuum dried, resuspended in 100 μL 1X OP50, and plated on 3 cm plates containing 3 mL NGM agar.

Nematode Lipid Extracts

Worms were grown on 10 cm NGM agar plates seeded with OP50 bacteria. Gravid adults were bleached and the resulting embryos transferred to liquid culture (S-complete medium supplemented with 100X concentrated OP50). Two to three rounds of growth and lysis were performed. For the final round, worms were grown at 20°C until the L3-L4 stage, harvested, frozen in liquid nitrogen and stored at -80°C. Thawed worms were homogenized and total lipids (plus 1 μg cholesterol-d_7 or chenodeoxycholic acid (CDCA)-d_4/10^7 worms) were extracted with 2:1 chloroform:methanol. The resulting organic phase was dried under nitrogen. For GC/MS/MS analysis, growth of worms was carried out on plates only.

LC/MS/MS Analysis

Samples were analyzed by LC/MS/MS using 6410 Triple Quadrupole LC/MS instrument (Agilent Technologies, Santa Clara, CA) equipped with an ESI source and a Zorbax XDB-C18 column (4.6 × 50 mm, 3.5 μm). Briefly, lipid extracts were resuspended in methanol, spiked with cholesterol-d_7 as an internal standard, and analyzed in Multiple Reaction Monitoring (MRM) mode. The following transitions were observed: cholesterol-d_7 (*m/z* 411→376) and 7-dehydrocholesterol (*m/z* 385→369).

GC/MS/MS Analysis

Samples were analyzed by GC/MS/MS on a 7000A Triple Quadrupole GC/MS instrument (Agilent Technologies, Santa Clara, CA) equipped with an ESI source and an HP-5MS column. Briefly, lipid extracts were spiked with cholesterol-d_7 or 5β-cholanic acid as internal standards and derivitized with (trimethylsilyl)diazomethane. Compounds were analyzed in MRM mode using the following transitions: cholesterol-d_7 (*m/z* 465.4→360.3), cholesterol (*m/z* 458.4→353.3), 7-dehydrocholesterol (*m/z* 350.2→195.0), 5β-cholanic acid (*m/z* 374.3→264.0) and Δ^7-dafachronic acid (*m/z* 428.3→229).

qRT-PCR

Real-time quantification for microRNAs by RT-PCR was performed with a protocol modified from a previous report (Chen *et al.* 2005). Briefly, total RNA was purified from L3 stage larvae using TRIzol (Invitrogen, Carlsbad, CA) and the miRNeasy kit (Qiagen, Hilden, Germany). TaqMan MicroRNA Reverse Transcription kit (Applied Biosystems, Carlsbad, CA) was used to generate cDNA with microRNA-specific primers. qRT-PCR was performed with Power SYBR Green master mix (Applied Biosystems, Carlsbad, CA) according to the manufacturer's instructions. Sno-RNA U18 was used as an internal control. The following primers were used: 5'-CAGTGCAGGGTCCGAGGT-3' (*U18-RT*); 5'-GGCAGTGATGATCACAAATC-3'(*U18*-f); 5'-TGGCTCAGCCGGTTTTCTAT-3' (*U18*-r); 5'-GTCGTATCCAGTGCAGGGTCCGAGGTATTCGCACTGGATACGACTCATTT-3' (*mir-241*-RT); 5'-CGCTGAGGTAGGTGCGAG-3' (*mir-241*-f); 5'-GTCGTATCCAGTGCAGGGTCCGAGGTATTCGCACTGGATACGACTACAAT-3' (*mir-84*-RT); 5'-GCGCGCTGAGGTAGTATGTAAT-3'(*mir-84*-f); 5'-GTGCAGGGTCCGAGGT-3' (microRNA reverse primer).

Statistical Analysis

Results are presented as mean ± SD or SEM, as indicated. P values were calculated where appropriate using GraphPad Prism (GraphPad Software Inc., La Jolla, California).

Supplementary Material

Refer to Web version on PubMed Central for supplementary material.

Acknowledgments

We thank Antebi lab members for manuscript comments. This work was supported by the NIA (RO1AG027498) and the Max Planck Society (A. Antebi); the Howard Hughes Medical Foundation, NIH (U19DK62434), and the Welch Foundation (D.J. Mangelsdorf); the Natural Sciences and Engineering Research Council of Canada (356873-08), the Canadian Institutes of Health Research (MOP-89361 and 97904), and the Canada Foundation for Innovation (C.L. Cummins).

References

Antebi A, Yeh WH, Tait D, Hedgecock EM, Riddle DL. *daf-12* encodes a nuclear receptor that regulates the dauer diapause and developmental age in *C. elegans*. Genes Dev. 2000; 14:1512–1527. [PubMed: 10859169]

Bethke A, Fielenbach N, Wang Z, Mangelsdorf DJ, Antebi A. Nuclear Hormone Receptor Regulation of MicroRNAs Controls Developmental Progression. Science. 2009; 324:95–98. [PubMed: 19342589]

Bugg TD, Ramaswamy S. Non-heme iron-dependent dioxygenases: unravelling catalytic mechanisms for complex enzymatic oxidations. Curr Opin Chem Biol. 2008; 12:134–140. [PubMed: 18249197]

Chen C, Ridzon DA, Broomer AJ, Zhou Z, Lee DH, Nguyen JT, Barbisin M, Xu NL, Mahuvakar VR, Andersen MR, Lao KQ, Livak KJ, Guegler KJ. Real-time quantification of microRNAs by stem-loop RT-PCR. Nucleic Acids Res. 2005; 33:e179. [PubMed: 16314309]

Chitwood DJ. Biochemistry and Function of Nematode Steroids. Crit Rev Biochem Mol Biol. 1999; 34:273–284. [PubMed: 10517647]

Dumas KJ, Guo C, Wang X, Burkhart KB, Adams EJ, Alam H, Hu PJ. Functional divergence of dafachronic acid pathways in the control of *C. elegans* development and lifespan. Dev Biol. 2010; 340:605–612. [PubMed: 20178781]

Gerisch B, Antebi A. Hormonal signals produced by DAF-9/cytochrome P450 regulate *C. elegans* dauer diapause in response to environmental cues. Development. 2004; 131:1765–1776. [PubMed: 15084461]

Gerisch B, Rottiers V, Li D, Motola DL, Cummins CL, Lehrach H, Mangelsdorf DJ, Antebi A. A bile acid-like steroid modulates *Caenorhabditis elegans* lifespan through nuclear receptor signaling. Proc Natl Acad Sci U S A. 2007; 104:5014–5019. [PubMed: 17360327]

Gerisch B, Weitzel C, Kober-Eisermann C, Rottiers V, Antebi A. A Hormonal Signaling Pathway Influencing *C. elegans* Metabolism, Reproductive Development, and Life Span. Dev Cell. 2001; 1:841–851. [PubMed: 11740945]

Glover M, Glover J, Morton RA. Provitamin D3 in Tissues and the Conversion of Cholesterol to 7-Dehydrocholesterol *in vivo*. Biochem J. 1952; 51:1–9. [PubMed: 14944524]

Hu Y, van der Geize R, Besra GS, Gurcha SS, Liu A, Rohde M, Singh M, Coates A. 3-Ketosteroid 9α-hydroxylase is an essential factor in the pathogenesis of *Mycobacterium tuberculosis*. Mol Microbiol. 2010; 75:107–121. [PubMed: 19906176]

Jia K, Albert PS, Riddle DL. DAF-9, a cytochrome P450 regulating *C. elegans* larval development and adult longevity. Development. 2002; 129:221–231. [PubMed: 11782415]

Kenyon CJ. The genetics of ageing. Nature. 2010; 464:504–512. [PubMed: 20336132]

Mak HY, Ruvkun G. Intercellular signaling of reproductive development by the *C. elegans* DAF-9 cytochrome P450. Development. 2004; 131:1777–1786. [PubMed: 15084462]

Motola DL, Cummins CL, Rottiers V, Sharma KK, Li T, Li Y, Suino-Powell K, Xu HE, Auchus RJ, Antebi A, Mangelsdorf DJ. Identification of Ligands for DAF-12 that Govern Dauer Formation and Reproduction in *C. elegans*. Cell. 2006; 124:1209–1223. [PubMed: 16529801]

Ogawa A, Streit A, Antebi A, Sommer RJ. A Conserved Endocrine Mechanism Controls the Formation of Dauer and Infective Larvae in Nematodes. Curr Biol. 2009; 19:67–71. [PubMed: 19110431]

Patel DS, Fang LL, Svy DK, Ruvkun G, Li W. Genetic identification of HSD-1, a conserved steroidogenic enzyme that directs larval development in *Caenorhabditis elegans*. Development. 2008; 135:2239–2249. [PubMed: 18495818]

Rottiers V, Motola DL, Gerisch B, Cummins CL, Nishiwaki K, Mangelsdorf DJ, Antebi A. Hormonal Control of *C. elegans* Dauer Formation and Life Span by a Rieske-like Oxygenase. Dev Cell. 2006; 10:473–482. [PubMed: 16563875]

Russell DW. The enzymes, regulation, and genetics of bile acid synthesis. Annu Rev Biochem. 2003; 72:137–174. [PubMed: 12543708]

Wang Z, Zhou XE, Motola DL, Gao X, Suino-Powell K, Conneely A, Ogata C, Sharma KK, Auchus RJ, Lok JB, Hawdon JM, Kliewer SA, Xu HE, Mangelsdorf DJ. Inaugural Article: Identification

of the nuclear receptor DAF-12 as a therapeutic target in parasitic nematodes. Proc Natl Acad Sci U S A. 2009; 106:9138–9143. [PubMed: 19497877]

Wollam J, Antebi A. Sterol Regulation of Metabolism, Homeostasis, and Development. Annu Rev Biochem. 2011; 80:885–916. [PubMed: 21495846]

Yoshiyama T, Namiki T, Mita K, Kataoka H, Niwa R. Neverland is an evolutionally conserved Rieske-domain protein that is essential for ecdysone synthesis and insect growth. Development. 2006; 133:2565–2574. [PubMed: 16763204]

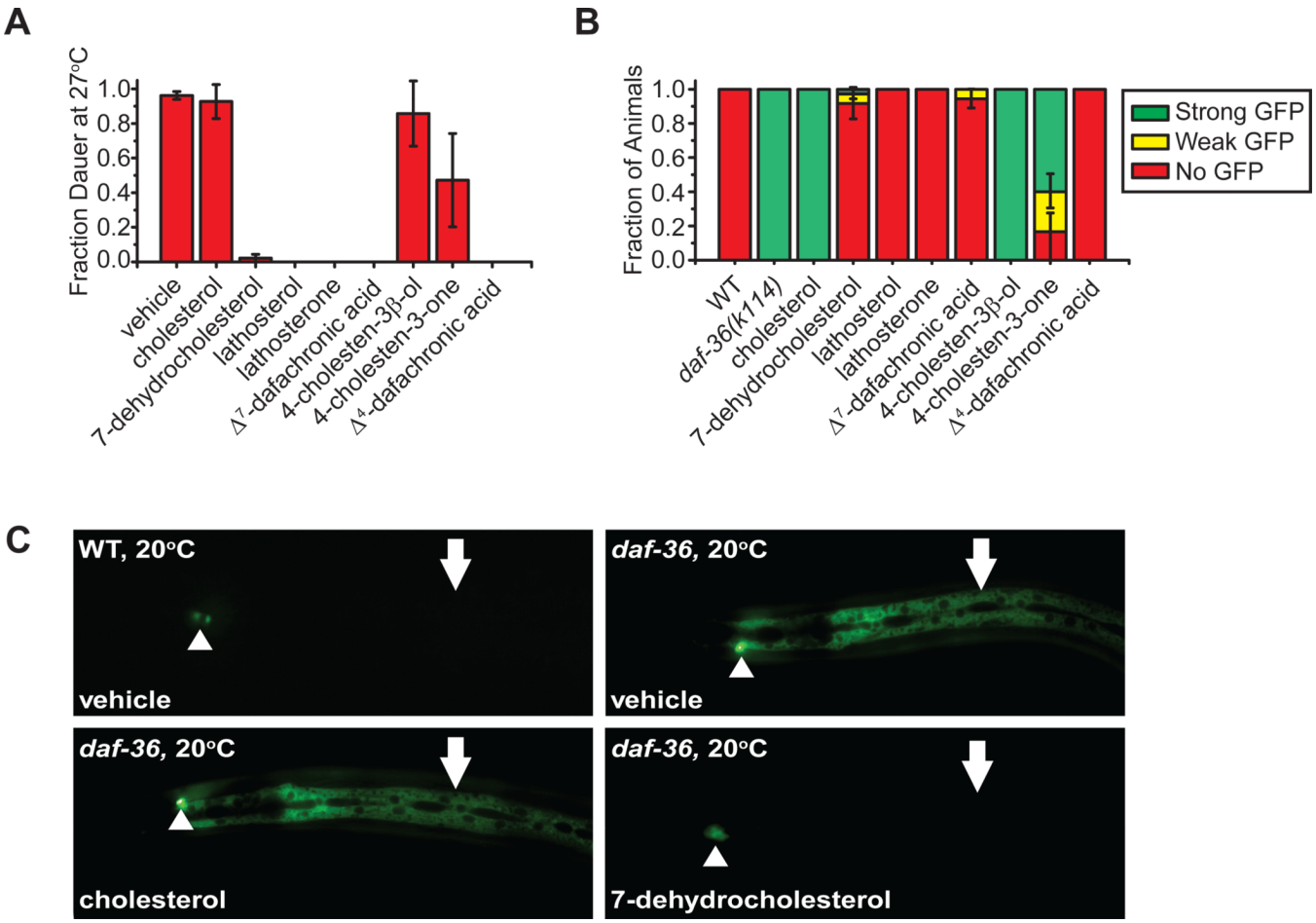

Figure 1. Rescue experiments suggest DAF-36 produces 7-dehydrocholesterol

(A) *daf-36(k114)* Daf-c phenotypes at 27°C are rescued with 7-dehydrocholesterol, the dafachronic acids (DAs) and all proposed precursors of the DAs, but not cholesterol. Partial rescue is seen with 4-cholesten-3-one. Experiments were carried out with a compound concentration of 33 μM and ethanol as the vehicle (N≥3, mean ± SD). (B) *daf-9::gfp* hypodermal expression is upregulated in *daf-36(k114)* mutants, suggesting loss of negative feedback on *daf-9* expression. 7-dehydrocholesterol and downstream DA precursors fully rescue this upregulation. The fraction of animals with strong (green), weak (yellow), or no (red) hypodermal GFP expression is shown (N≥3, mean ± SD). (C) N2 wild-type (WT) and *daf-36(k114)* animals expressing *daf-9::gfp*. Arrowheads indicate the XXX R/L neuroendocrine cells in which *daf-9* expression is relatively unchanged, and arrows indicate hypodermal expression.

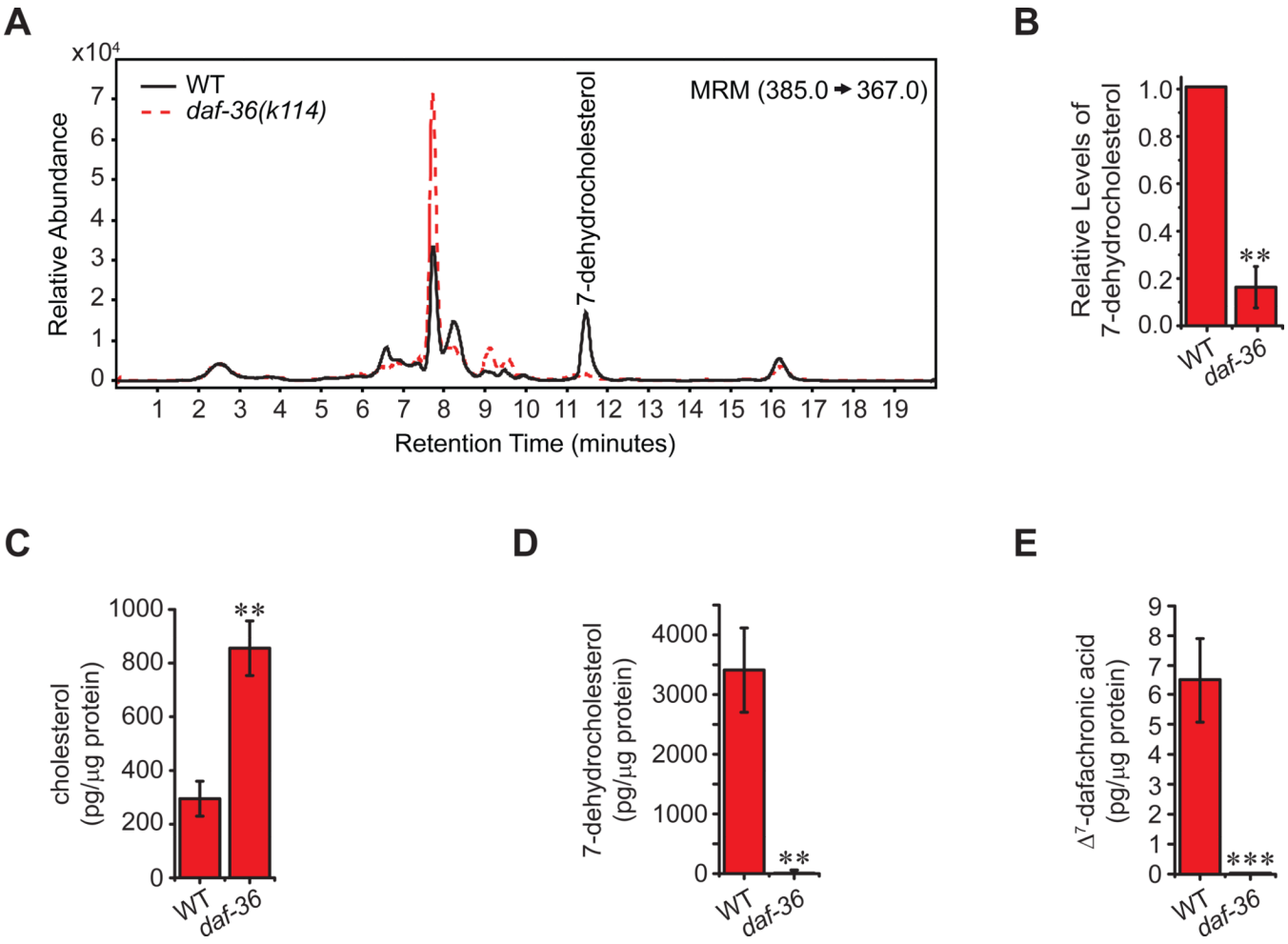

Figure 2. *daf-36* mutant animals are deficient in 7-dehydrocholesterol

(A) LC/MS/MS analysis of lipid extracts from L3 stage animals reveals that 7-dehydrocholesterol levels are significantly reduced in *daf-36(k114)* mutant animals relative to N2 wild-type (WT) animals, shown quantitatively in (B) (N=4, mean ± SEM, ***P*<0.005, determined by paired t-test). (C) Analysis of *daf-36* lipid extracts by GC/MS/MS shows that cholesterol levels are significantly elevated, whereas animals are deficient in (D) 7-dehydrocholesterol and (E) Δ^7-DA (N=5, mean ± SEM, ***P*<0.005, determined by unpaired t-test, ***below limit of detection).

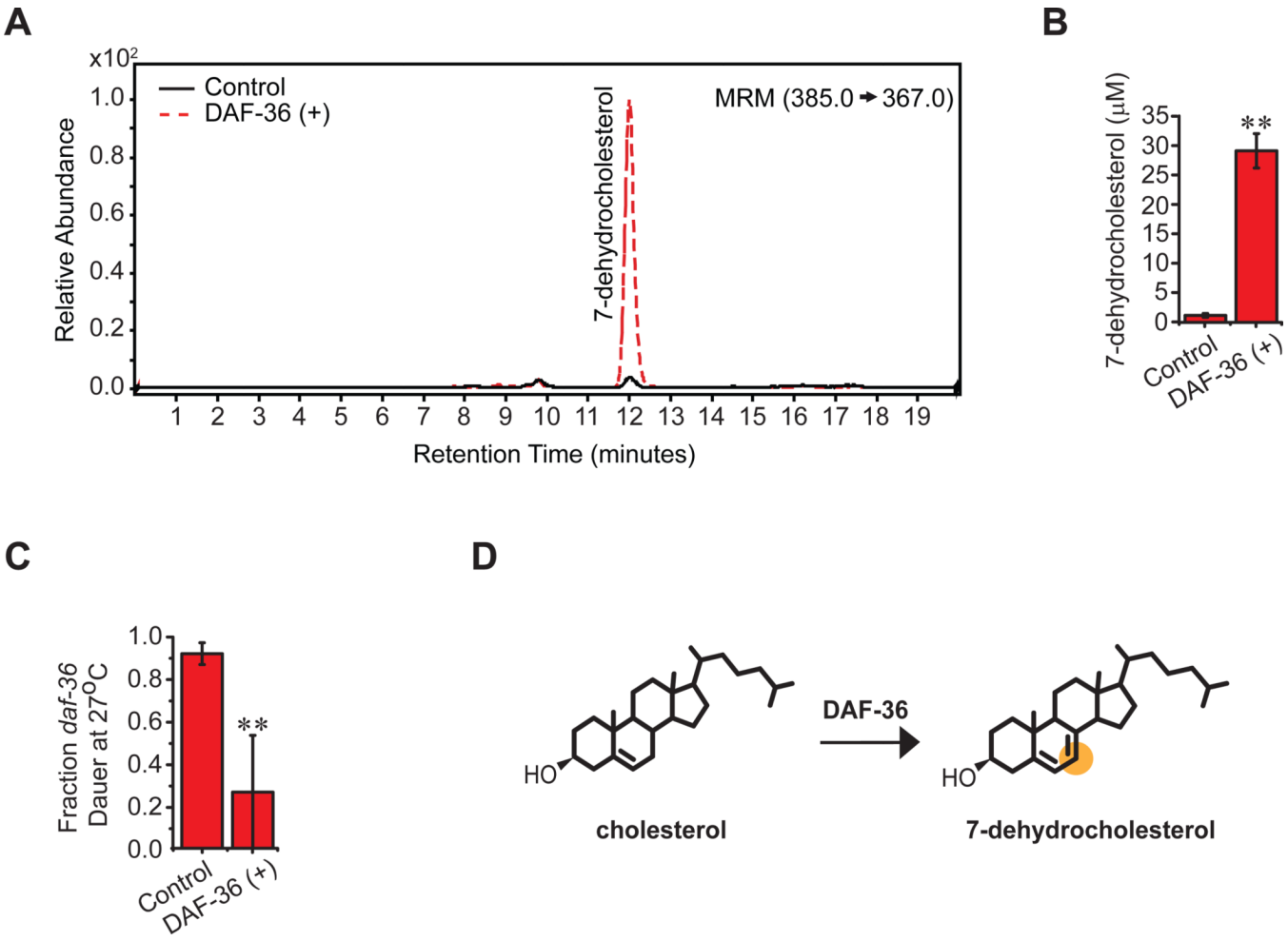

Figure 3. DAF-36 produces 7-dehydrocholesterol

(A) LC/MS/MS scans of lipid extracts from microsomes expressing either human CYP450 oxidoreductase (hOR) (Control) or DAF-36+hOR (DAF-36(+)), showing that production of 7-dehydrocholesterol is detected in the presence of DAF-36, whereas it is absent in control microsomes, shown quantitatively in (B) (N=3, mean ± SEM, ***P*<0.001, determined by unpaired t-test). (C) Supplementation of *daf-36(k114)* with lipid extracts from microsomes expressing human CYP450 oxidoreductase (hOR) (Control) or DAF-36+hOR (DAF-36 (+)) shows DAF-36 and 7-dehydrocholesterol dependent rescue of dauer formation at 27°C (N=2, mean ± range, ***P*<0.001, determined by Fisher's exact test of grouped data). (D) DAF-36 acts as a cholesterol 7-desaturase, introducing a double bond at the 7 position, forming 7-dehydrocholesterol, shown highlighted in orange.

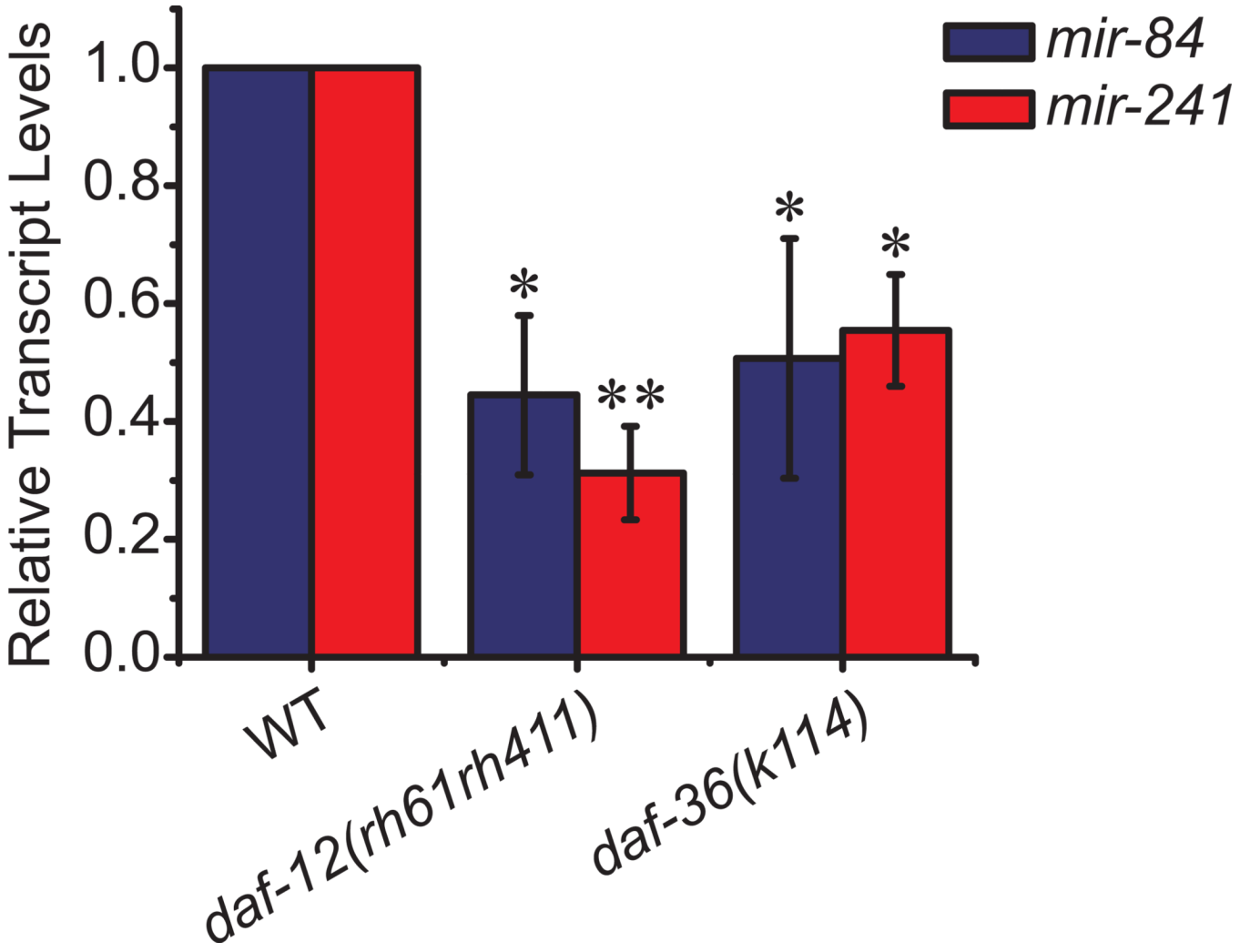

Figure 4. Loss of *daf-36* impacts DAF-12 activity

daf-36(k114) mutant animals have significantly lower transcript levels of two known targets of DAF-12, *mir-84* and *mir-241*, relative to N2 wild-type (WT) animals, determined by quantitative RT-PCR of L3 stage worms. This reduction is similar to that seen in *daf-12(rh61rh411)* null mutants (N=3, mean ± SD, **P*<0.05, ***P*<0.005, determined by unpaired t-test).